FLUORESCENCE-BASED NANOTHERMOMETRY:
SYNTHESIS AND CHARACTERIZATION OF DYED SILICA NANOPARTICLES AS THERMAL SENSORS

GRADO EN FÍSICA

Arnau Company Pascual

Tutores académicos:

Paul Eduardo David Soto Rodríguez

Inocencio Rafael Martínez Benenzuela

Junio 2024

ABSTRACT

Fluorescence-based thermometry is a field of great scientific and technological interest due to its ability to take accurate, remote and non-invasive measurements. However, its most outstanding feature is its viability for measurement at the nanoscale, especially in areas such as nanoelectronics or biomedicine.

This work proposes the development of a thermal nanosensor by encapsulating two fluorescent compounds in the matrix of silica nanoparticles and studying the variations of their luminescence with temperature changes. This study describes the processes used to synthesize the particles and functionalize them with two fluorescent organic dyes: Rhodamine B and Fluorescein Isothiocyanate.

After the preparation of the particles, the variations of their emission spectra with temperature changes in the biological range are studied. In particular, the changes of the intensities of the emission bands of the compounds are analyzed, allowing the calibration and temperature measurements to be obtained. The sensor's sensitivity is discussed, and its performance is compared to other similar sensors. Afterwards, a temperature uncertainty study is made to prove the reliability of the sensor.

Finally, based on the development and the results obtained, a series of improvements are proposed, along with alternative approaches to the preparation of the sensor for its potential use in biomedical applications.

RESUMEN

La medición de la temperatura basada en fluorescencia es un área de gran interés científico y tecnológico debido a su capacidad de tomar medidas precisas, remotas y no invasivas. Sin embargo, su característica más destacable es su viabilidad para la medición a escala nanométrica, especialmente en áreas como nanoelectrónica o biomedicina.

Este trabajo propone el desarrollo de un sensor térmico a nanoescala encapsulando dos compuestos fluorescentes en la matriz de nanopartículas de sílice, y estudiando las variaciones de su luminiscencia con los cambios de temperatura. Para ello, se explican los procesos seguidos para la síntesis de dichas partículas, así como para su funcionalización con dos compuestos orgánicos fluorescentes: *Fluorescein isothiocyanate* y *Rhodamine B*.

A partir de la formación de las partículas, se estudian las variaciones de su espectro de emisión con los cambios de temperatura en el rango biológico. Específicamente, se analizan los cambios en las intensidades de las bandas de emisión de los compuestos, a partir de los cuales se realiza una calibración para obtener medidas de la temperatura. Se discute la sensitividad del sensor y se compara su rendimiento al de otros sensores parecidos. Posteriormente, se hace un estudio de los posibles errores en la medición.

Finalmente, en base al desarrollo y a los resultados obtenidos, se proponen líneas de mejora, así como distintas propuestas para la preparación del sensor para su posible uso en aplicaciones biomédicas.

Contents

Chapter 1

Introduction

RESUMEN: En este capítulo, se introducen los conceptos en los que se basará el estudio. Se detalla la importancia de la medición de la temperatura a nanoescala, y cómo los sensores basados en fluorescencia son una propuesta prometedora para aplicaciones biomédicas. Finalmente, se profundiza en los distintos ámbitos necesarios para el desarrollo del sensor: dependencia de la luminiscencia de un material con la temperatura, tipos de materiales fluorescentes y el uso de nanopartículas para encapsular dichos materiales.

Temperature (T) is one of the most important physical parameters to study for humankind, it manifests in daily people's lives as well as in many fields of science and technology. This makes temperature measurements a relevant area of focus for the scientific community, resulting in the development of new techniques to be adapted to challenges presented by recent technology advancements. Consequently, there is a growing need for temperature sensing at nanoscale due to the increasing interest in the development of micro- and nanometer scale systems, specifically in fields such as micro/nanoelectronics or biomedicine [1].

Focusing on the biomedicine field, in biological systems the changes of the local temperature plays an important role on the system dynamics and its properties [2]. For example, cancer cells have larger inter cellular temperatures than healthy ones due to higher metabolism activity [3], therefore being able to detect these changes will be of great interest for early cancer detection. To achieve the sensing of this kind of local temperature changes, luminescence-based thermometry has emerged as an attractive experimental tool for many investigations thanks to its capacity to take precise, remote and non-invasive measurements. Being around 10 μm the typical cell size [4], using temperature sensors at the nanoscale would be a great asset to study these systems [5].

Fluorescence of a given substance can be explained as the emission of light due to the population decay of the electronic states of the material excited by an external source. Some energy properties of the electronic states are temperature-dependent, consequently,

temperature changes in the material will be reflected in changes on its fluorescence emission spectrum, such as variations in intensity, band shape or life-time, among others [6]. These variations can be calibrated to create a temperature sensor based on the given material's luminescence. In this work we focus on the changes of the intensities of the emission band, which are the most sensitive to temperature variations and, consequently, the most used to create thermal sensors. It was seen that using a single optical transition band as a main element to design a temperature sensor leads to several problems, more precisely the measurements can be affected by many factors, such as environmental changes, photobleaching of the sample, or drifts of the optoelectronic system [5], [7], [8]. Therefore, using two transition bands would be of interest as it would allow to form a ratiometric intensity measurement scheme, which avoids the before mentioned problems. The path followed in this work to achieve a system of this type was to synthesize nanoparticles which could permit the encapsulation of two fluorophores in their matrix.

One important matter to discuss if biomedical applications are considered is the sensor's biocompatibility, so the sensor itself shouldn't interfere in the state of the biological system or its components (cells or tissues). For that reason, silica (SiO_2) particles have been chosen to be the sensor's host material, because, despite the toxicity of silica nanoparticles depends on many factors, such as the particles size, the exposure dose or the type of tissue or cell to be treated [9], [10]; many works have confirmed its biocompatibility and used them to study the treatment of different diseases [11], [12]. In addition to other biocompatibility, silica particles are a focus of interest for biological applications for other reasons like controllable particle size, large surface area that permits various kinds of functionalization, good physical stability, and chemical inertia.

Moreover, core-shell structure particles have recently attracted great attention due to their capacity to control the particles' properties, with new possibilities such as combining different materials or modifying the particles' surface [13]. These structures can be useful in ratiometric thermometers, being able to encapsulate two luminescent sources in a single particle. In specific, previous works successfully use silica nanoparticles with a core-shell structure for dye encapsulation in sensing applications [14], [15].

Many fluorescent materials have been used to make luminescence nanothermometry, including lanthanide ions, quantum dots, luminescent organic dyes, luminescent polymers, among others. In this study, organic dyes will be used due to the facility of their functionalization with silica nanoparticles, which will be explained later in the work. In addition to the knowledge that they have an effective quantum yield, they are relatively affordable, and

they can be excited in the visible range, which makes the measurements more practical. The organic dyes chosen to be the luminescence source of the sensor created in this work were Fluorescein Isothiocyanate (FITC) and Rhodamine B. In general terms, the intensity of luminescence of organic dyes decreases when temperature increases due to the rise of the probability of non-radiative de-excitation processes [7]. That is the case with Rhodamine B, which has been widely used for its temperature dependent fluorescence intensity [16]. On the other hand, FITC's fluorescence intensity has been studied for its sensitivity with pH [17] but its behavior with temperature changes is not clear, it can be temperature-dependent but no strong correlation to the temperature has been found. Therefore, it is likely that the fluorescence intensity of FITC is influenced by other environmental properties of the system [18], [19].

Based on this information, in this work we report our attempt to create a functional fluorescence based ratiometric thermal sensor, synthesizing mesoporous core-shell silica nanoparticles, encapsulating two organic dyes in their matrix, and using its luminescence emission to calibrate it with the temperature.

Chapter 2

Methodology

RESUMEN: En este capítulo se comentan los procesos llevados a cabo para desarrollar y caracterizar el sensor, así como los materiales y equipos que han sido utilizados. Este desarrollo se divide en tres fases: la síntesis de las partículas, su funcionalización con los compuestos fluorescentes escogidos, y su posterior caracterización. Las partículas fueron sintetizadas con una estructura *core-shell* con la superficie mesoporosa. Posteriormente, se comenta cómo los compuestos orgánicos *Fluorescein isothiocyanate* y *Rhodamine B* fueron encapsulados en las partículas obtenidas. Finalmente, se describen las diferentes técnicas utilizadas para el análisis de los resultados.

Materials: Tetraethylorthosilicate (TEOS, 98%, Sigma-Aldrich), cetyltrimethylammonium bromide (CTAB), triethanolamine (TEOA), 3-aminopropyltriethoxysilane (APTES, ≥98%, Sigma-Aldrich), ethanol (EtOH), fluorescein isothiocyanate (FITC) (isomer I suitable for protein labeling, ≥90% (HPLC), Sigma-Aldrich), Rhodamine B. All chemicals were analytical-grade reagents. Deionized water (18.2 $M\Omega$) was used throughout the experiments.

It is worth explaining that the major focus point of this work is in the experimental setup, so it is divided in three separate parts: the nanoparticles synthesis, their functionalization with the organic dyes, and its later optical characterization. This scheme implies that each part's results must be satisfactory to obtain the desired outcome. The steps followed in each phase are explained in the following paragraphs, with their complications and the final methodology employed.

2.1 Synthesis

In the introduction, the benefits of using silica nanoparticles were argued, its versatility being one of their best. Also, the interest in using core-shell structures was mentioned. The idea in this section is to obtain nanoparticles that can be hosts of two fluorophores, to achieve this,

the particles synthesized had a mesoporous core-shell structure (SiO_2@mSiO_2) with a solid silica sphere in the center and with a mesoporous silica surface around it. The mentioned idea of encapsulating one dye in each layer (one in the core and one in the shell) was tested but the result wasn't satisfactory, for this reason we opted for using the porous structure of the surface to encapsulate one organic dye while the other was later attached to the surface using a silane, process that will be explained in detail further on.

Core: The solid SiO_2 spheres were synthesized via Stöber Method with some modifications [20]. This method allows the synthesis of particles with sizes between 50nm to 2μm, the materials are chosen to obtain results below 1 μm. A mixture with deionized H_2O (10 mL), EtOH (7 mL), and an NH_3:H_2O solution (25%, 2 mL) was stirred for 15 mins at room temperature, which ensures a homogeneous mixture. The ammonia solution acts here as a catalyst for TEOS hydrolysis. Then TEOS, the precursor of silica, was added dropwise (6 mL) and the mixture was left stirring for 24 hours for the hydrolysis and condensation of TEOS, leading to the formation of SiO_2 solid spheres. The particles obtained were collected by centrifugation, to separate the solid particles and the remnant liquid, and then were washed with EtOH 3 times to remove any residual impurities.

Mesoporous shell: To proceed to grow the mesoporous shell, the solid SiO_2 particles obtained in the previous step (60 mg) were dissolved in a mixture with H_2O (20 ml), TEOA (40 ml) and CTAB (80 mg), which is as a surfactant whose molecules act as a soft-template of the porous structure [9]. The solution was stirred at 80^{o}C for 10 minutes, then TEOS (0.125 ml) was added dropwise and the mixture was stirred for 2 hours. The resulting SiO_2@mSiO_2 particles were washed with EtOH and H_2O to remove the residues. After that, the resulting particles were calcinated to 600^{o}C. The calcination is necessary to remove the CTAB and obtain the mesoporous structure, furthermore, it removes organic residues and impurities, which results in a clean and reactive surface [21]. It also helps to obtain more hydrophilic OH^- groups, which can easily react with silanes such as APTES, that will be later used for the functionalization [22].

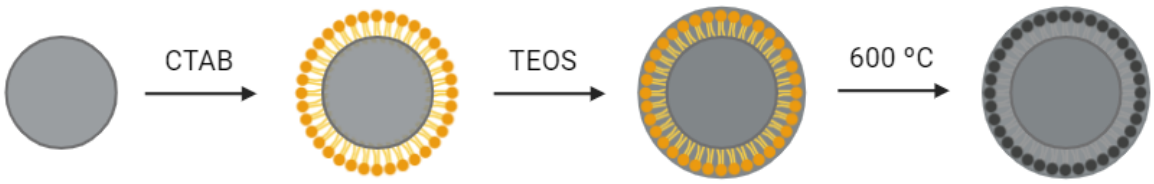

Figure 2.1: Graphical scheme that illustrates the growth of the outer mesoporous layer.

2.2 Functionalization

The functionalization was done in two steps, one for each organic dye. Rhodamine B was diffused into the porous structure of the particles, while FITC was attached to the particle's external layer using APTES. This is possible because APTES is a silane that can modify the surface of the silica introducing amino groups (-NH_2), which allows the reaction with the isothiocyanate groups (-N=C=S) of the FITC [23]. This scheme gives a homogenous structure of the dyes in the particles and makes full use of their entire surface area, which ensures the efficiency of each particle's fluorescence.

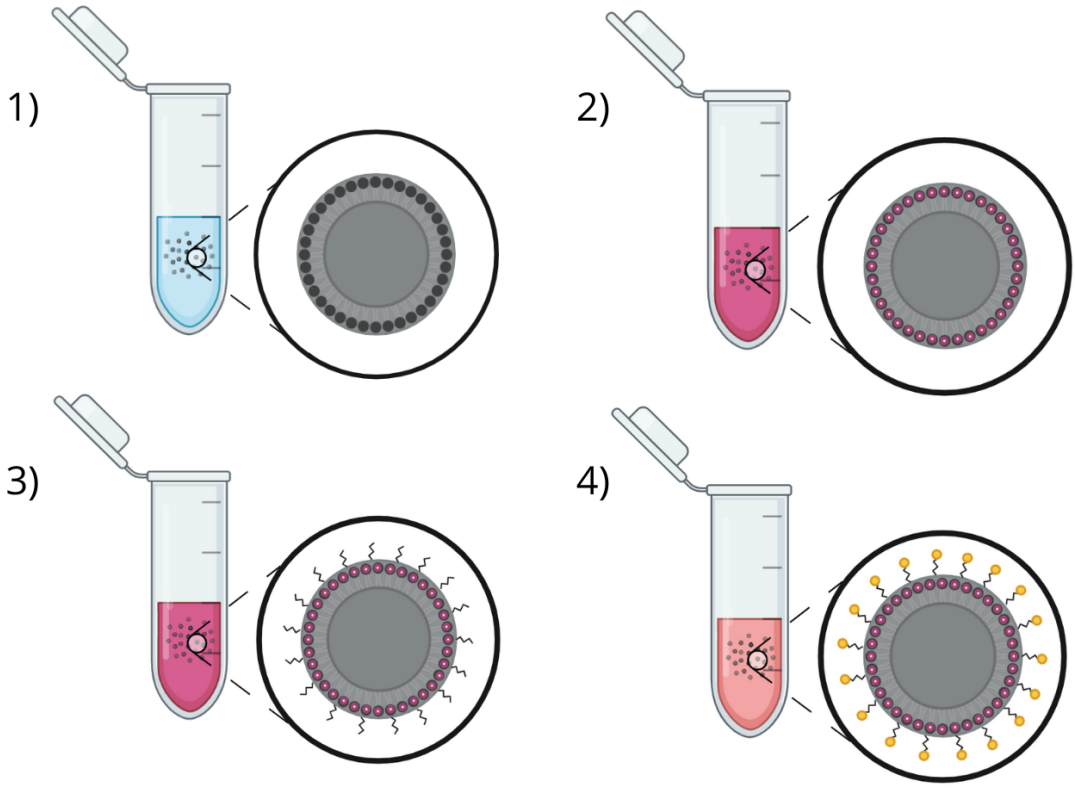

Figure 2.2: Graphical scheme of the functionalization process. 1) Particles in water solution. 2) Diffusion of Rhodamine B into the porous. 3) Addition of APTES. 4) Attachment of FITC into the surface.

The following procedure, also shown in Figure 2.2, was employed. First, Rhodamine B and FITC were suspended in a 1mg/ml water solution, when we refer to the organic dyes later on, we will be referring to these solutions. Then, the obtained core-shell SiO_2@mSiO_2 nanoparticles (7.5 mg) and Rhodamine B (80 μl) were suspended in H_2O (1 ml) and kept

stirring for 72 hours at room temperature for the rhodamine molecules to diffuse into the particle's porous. Later, APTES (50 μl) and FITC (10 μl) were added to the solution and stirred for 72 hours to create the bond particles-APTES-FITC. Afterwards, the resulting particles were washed several times with EtOH and H_2O to remove the residual APTES, FITC and Rhodamine B. Finally, the functionalized particles were dissolved in H_2O with a 1.875 mg/ml concentration for later characterization, so the measurements for the sensing are taken in an aqueous solution.

2.3 Characterization

Due to the nature of this study, various types of characterization are necessary to analyze the results properly. We opted for Transmission Electron Microscopy (TEM) to study the particles' synthesis results. In this method, an accelerated electron beam crosses the sample and interacts with it, then the transmitted electrons are collected by a detector, which transforms the electron signal into a visible image. TEM microscope JEOL JEM 2100 was used for the measurements.

To verify the functionalization, the absorption spectrum of the resulting particles was taken with a Cary Series UV-Vis-NIR Spectrophotometer (Agilent Technologies). This method employs a process that quantifies the light absorbed by the sample at different wavelengths. It is known that organic dyes have specific absorption bands, so if these are observed in the measurement, it can be supposed that the functionalization was successful. The sample was placed in a 3ml cuvette, the absorption of the cuvette and the water were corrected in the resulting absorption spectrum.

An FLS 1000 Photoluminescence Spectrometer (Edinburgh Instruments) was used to study the luminescent emission spectra of the functionalized particles. In this equipment, the light generated in a Xenon Lamp passes through a double monochromator with a 0.2nm spectral resolution, and then the light excites the sample at the selected wavelength. The fluorescence light emitted by the sample passes through another double monochromator before reaching the detector, see Figure 2.3.

Figure 2.3: Photoluminiscence spectrometer images. 1) 450 W Ozone-free Xenon Lamp. 2) Excitation monochromator (Czerny-Turner). 3) Sample holder. 4) Emission monochromator (Czerny-Turner). 5) Detector (PMT-900 Photomultiplier). Source: Edinburgh Instruments [24]

The sample was placed in a 3 ml cuvette for the measurements. The cuvette holder is equipped with a temperature-controlling system with an external fluid circulator. The *Fluoracle* software was used to control the equipment.

Chapter 3

Results and discussion

RESUMEN: En esta sección se presentan los resultados obtenidos de los métodos comentados anteriormente. Las imágenes TEM demuestran los resultados satisfactorios de la síntesis, mientras que se comprueba la correcta encapsulación de los compuestos orgánicos mediante los espectros de absorción y emisión de las partículas. Por otra parte, se detalla el estudio del comportamiento de la fluorescencia con la temperatura y la viabilidad del uso de las partículas como sensor térmico, obteniendo su sensitividad relativa y estimaciones del error.

This chapter will present the results obtained and discuss the potential use of the characterized particles as a thermal sensor for biological applications.

3.1 Synthesis and Functionalization

TEM Images show the particles resulting from the synthesis after calcination but before the encapsulation of the dyes, see Figure 3.1. The particles exhibit a monodisperse spherical shape, with a size between 150-200nm. While the pores are relatively visible in the last image, additional characterization techniques such as high-resolution X-ray diffraction or gas adsorption analysis (BET) would be necessary to determine the pore size, which is typically 2-5 nm [20]. This was not taken into account in this study, as the incorporation of the dyes into the particles is well reflected in the other results presented in the work.

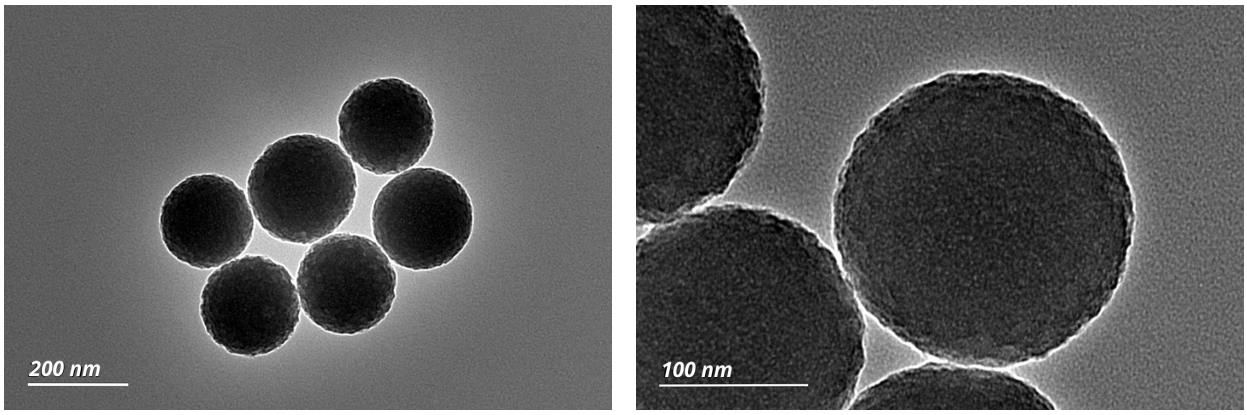

Figure 3.1: TEM images of SiO_2@mSiO_2 nanoparticles.

Focusing now on the results that allow us to check the functionalization, the absorption spectrum of the particles is shown in Figure 3.2. The spectrum is compared with the typical absorption bands of FITC [21] and Rhodamine B [25].

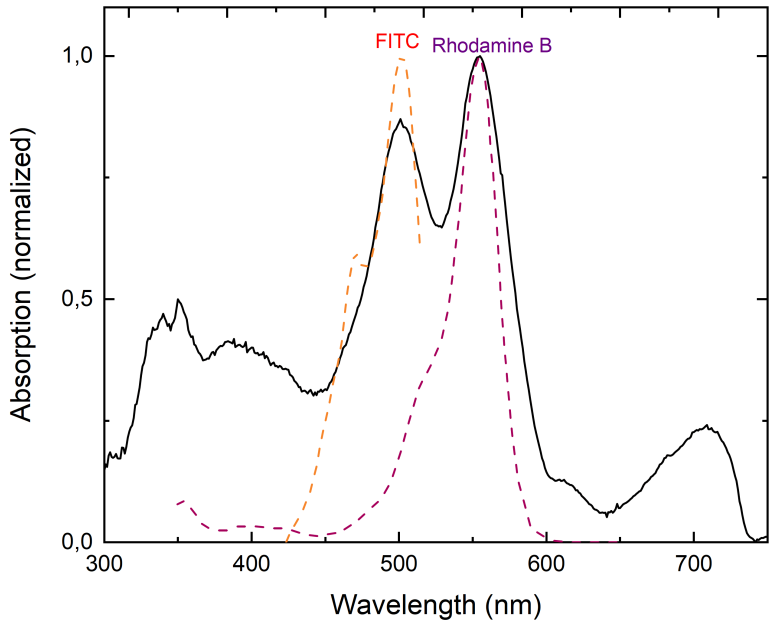

Figure 3.2: Absorption spectrum of the functionalized particles (black). Absorption bands of FITC (orange) and Rhodamine B (purple).

The most significant data correspond to the two bands observed with maxima at 500nm and 554nm, which coincide with the corresponding peaks of the two dyes. Some studies [19], [26] had proposed that if the distances between the dyes are sufficiently small (1-10 nm), a Förster Resonance Energy Transfer (FRET) process would happen. In this process,

the excited-state donor molecule transfers energy in a non-radiative form to a proximal acceptor donor molecule. In our case, under excitation at 470 nm, FITC would be the donor and Rhodamine B would be the acceptor. In our system, this process could happen, but since the Rhodamine B molecules are inside the shell's porous and the FITC molecules are outside, it can be assumed that the mean distance between the dyes' molecules is greater than 10 nm. However, this matter should be investigated in future works. Assuming this approach, FRET would not be the primary energy transfer mechanism, but instead, the FITC fluorescence emission would produce the excitation of the Rhodamine B molecules, resulting in a two-band emission spectrum. This can be seen in Figure 3.3. Considering the absorption spectrum, 470 nm seems an appropriate wavelength to excite the sample.

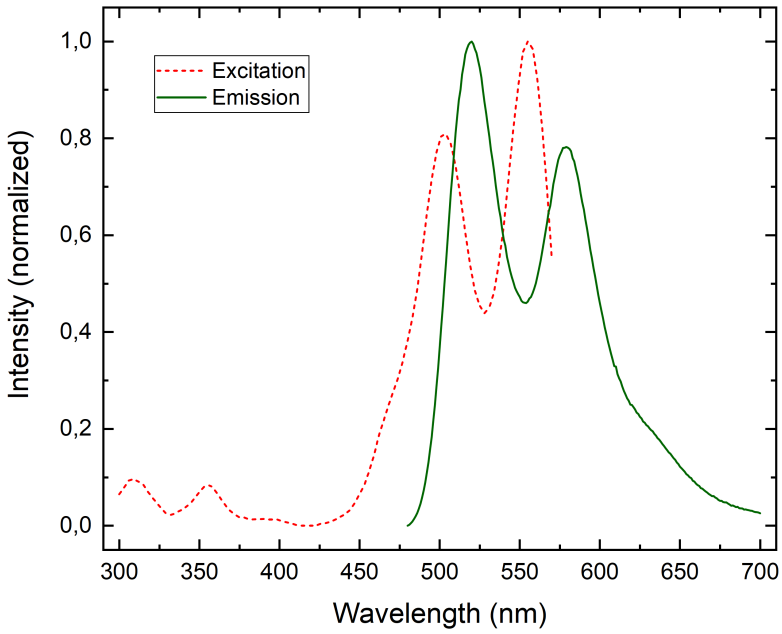

Figure 3.3: Excitation spectrum ($\lambda_{em} = 580$ nm), and emission spectrum of the sample at room temperature ($\lambda_{exc} = 470$ nm).

Following the analysis of the absorbance, the fluorescence emission of the particles at room temperature was measured. Figure 3.3 illustrates the excitation and emission bands of the respective organic dyes, with the FITC peak centered at 520 nm, while the Rhodamine B peak is at 580nm. Absorption bands coincide with the excitation ones, which is an expected outcome. These results confirm the efficacy of the functionalization process.

3.2 Ratiometric thermometry

A series of emission measurements were taken at different temperatures in the range 20-70ºC. The Figure 3.4 shows a strong temperature dependence in both emission peaks. A slight redshift can be observed in the FITC emission peak, while in the Rhodamine's a ≈5nm blueshift is perceived. The 580 nm emission intensity decreased mostly in the 20-50ºC range, and the 520 nm emission intensity increased in the 50 to 75ºC range. Rhodamine B temperature quenching behavior has been studied, its intensity decreases almost linearly with the temperature in the biological range [7]. On the other hand, the luminescence behavior of FITC, as it was said in the introduction, may be unstable with temperature changes. Moreover, it is important to mention that FITC is sensitive to pH variations, and it should be taken into account that the particles are in a neutral pH solution.

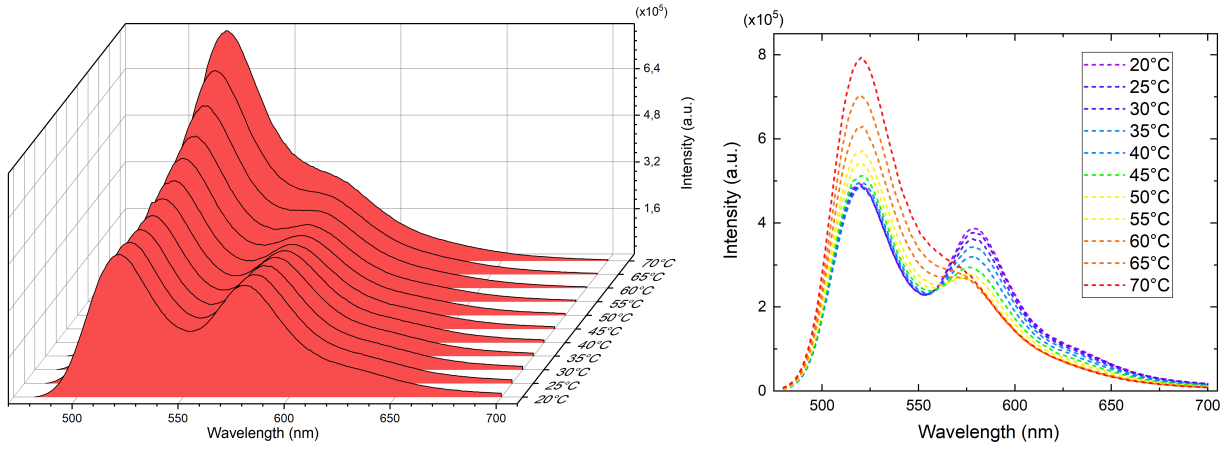

Figure 3.4: Temperature dependent emission spectra of the FITC and Rhodamine B dyed silica nanoparticles.

In the ratiometric thermometry method, two wavelengths must be chosen to study their temperature dependence. These wavelengths don't need to be the emission maximum values, but each wavelength must be in each fluorophore band. By dividing the 20 and 70ºC spectra, the wavelengths with the maximum ratio change has been selected. Therefore, 544nm and 591nm wavelengths were chosen to calculate the emission intensity ratio and its temperature dependence, see Figure 3.5.

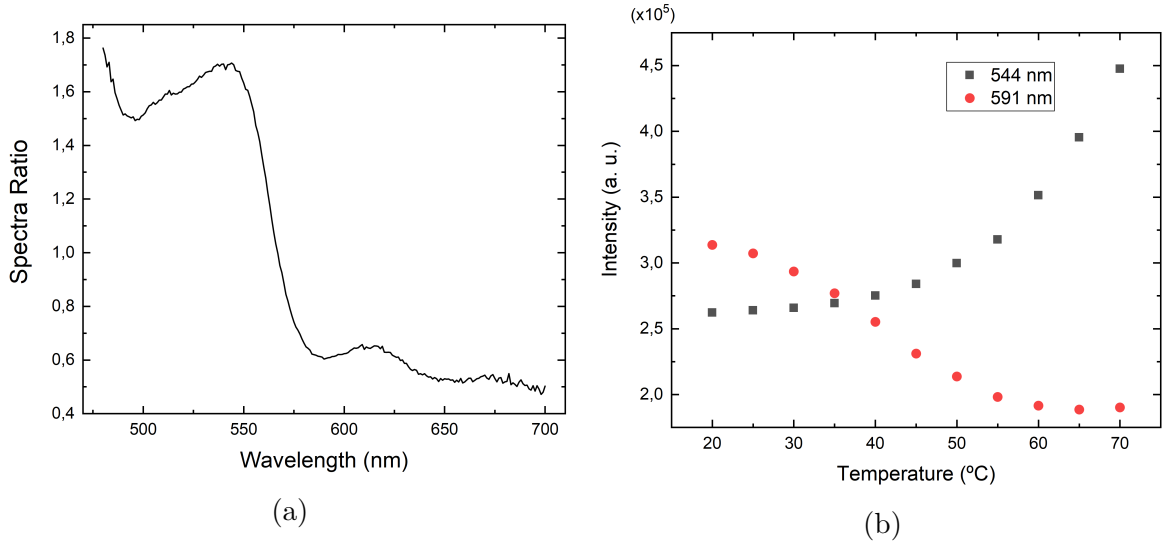

(a) (b)

Figure 3.5: (a) Graph obtained dividing 70ºC and 20ºC spectra. (b) Intensity values at 544nm and 591nm as a function of temperature.

There are several cases where the behavior of fluorophore emission intensity with temperature can be predicted, such as the case of lanthanide ions, whose thermally coupled energy levels are governed by the Boltzmann equation. In this work this model is not applied, so there are environmental factors that should be further studied to provide a predictive model. For this reason, the calibration of the intensity changes with temperature has been fitted to the equation indicated in Figure 3.6.

As the fluorescence-based thermometry field is progressing, more and more ways to prove the reliability of temperature sensors are applied. In this work, relative sensitivity is used to prove the measuring capacity of the sensor. Relative sensitivity S_{rel} is defined by the Eq (3.1), with R being the emission intensity ratio in the selected wavelengths, in this case I_{591nm}/I_{544nm}. This parameter, often represented as a percentage, indicates the relative change of the intensity ratio per degree, so the higher the parameter, the better the sensor's ability to detect temperature changes.

$$S_{rel} = \frac{1}{R}\left|\frac{dR}{dT}\right| \cdot 100 \tag{3.1}$$

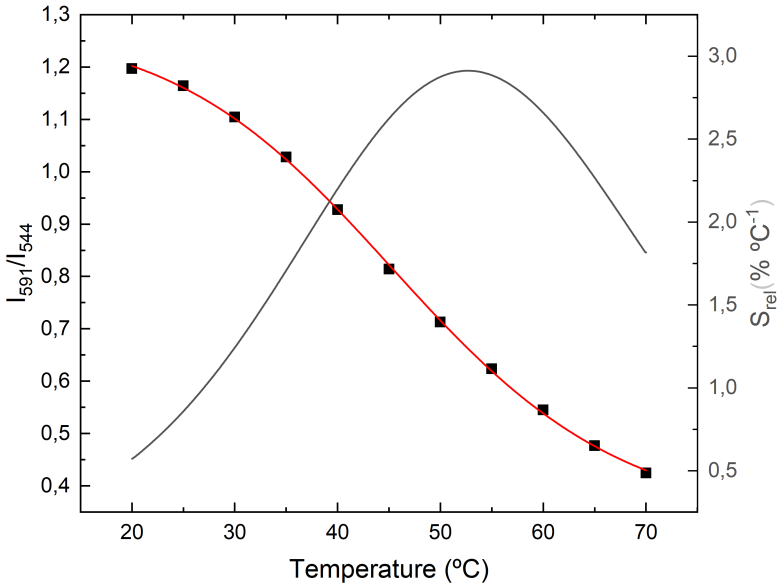

Figure 3.6: Experimental intensity ratio R (black squares) and relative sensitivity (S_{rel}) (grey line). R points were fitted to the equation $R = \frac{1.22-0.23}{1+(T/49.35)^{4.04}} + 0.23$.

In Figure 3.6, the S_{rel} curve is shown with an amplitude between 0.6-2.91%ºC^{-1}, being 51ºC the temperature with the maximum relative sensitivity. Along the measured range (27-70ºC), the relative sensitivity is $\geq$1%ºC^{-1}, which is considered a high sensitivity and feasible for biological applications [5]. In addition, a performance comparison of the sensor's results is given in Table 3.1, which shows the properties of other ratiometric thermal sensors formed by nanoparticles that encapsulate two organic dyes. The sensor developed and studied in this work shows good results maintaining a good relative sensitivity in the biological range. Altogether, considering the biocompatibility of mesoporous silica nanoparticles, the sensor shows potential to be used for biological applications.

Table 3.1: Performance comparison of different luminescent nanothermometers with encapsulated organic dyes as fluorescence sources.

Particles	Size [nm]	Organic dyes	T range [ºC]	S_{rel} [%ºC^{-1}]	Ref.
F127-melamine-formaldehyde polymer	88–105	Rhodamine 110/ Rhodamine B	20-90	7.6	[27]
γ-cyclodextrin MOFs	500-700	Fluorescein/ Rhodamine B	10-50	3.9-5.1	[28]
$mSiO_2$	40-60	FITC/ Rhodamine B	25-45	0.2-3	[19]
SiO_2@$mSiO_2$	180-200	FITC/ Rhodamine B	20-70	0.6-2.91	This work
F127 polymer	45-50	TBB/ Rhodamine 110	20-70	2.37	[29]
DLPC and DMPC nanocapsules	200	Rhodamine 110/ Indocyanine green	20-85	1.7	[30]
$mSiO_2$	30-70	Rhodamine 6G/Rhodamine B	20-50	1	[31]
ZIF8 MOFs	300	4-methylumbelliferone/Fluorescein	60-240	0.68	[32]

Temperature resolution (or uncertainty) δT is another crucial parameter to determine the

thermometer reliability. To make an estimation of the temperature uncertainty [33], 100 measurements of the sample were taken at 20, 40, and 60^{o}C. The fitting equation of the intensity ratio was used to obtain the corresponding temperature measurements, and the uncertainty estimation would be the standard deviation of the temperatures obtained, shown in Figure 3.7.

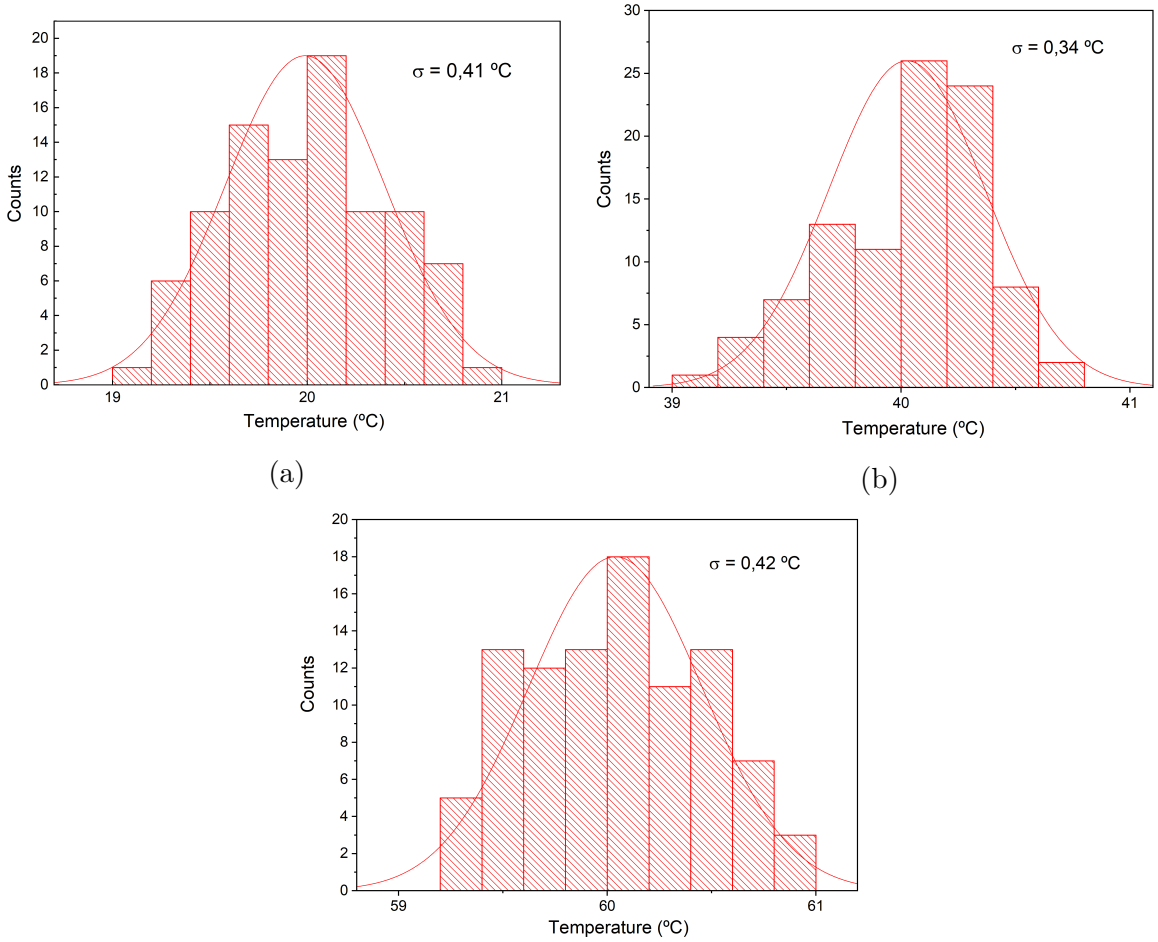

Figure 3.7: Temperature distributions and standard deviations of 100 measurements at (a) 20, (b) 40 and (c) 60^{o}C.

In addition, to make a theoretical estimation of the temperature resolution in all the measured range, δT was calculated using Eq (3.2), where δR is the uncertainty of the emission ratio taken as the standard deviation of the 100 measurements at 20^{o}C.

$$\delta T = \frac{1}{S_{rel}} \frac{\delta R}{R} \tag{3.2}$$

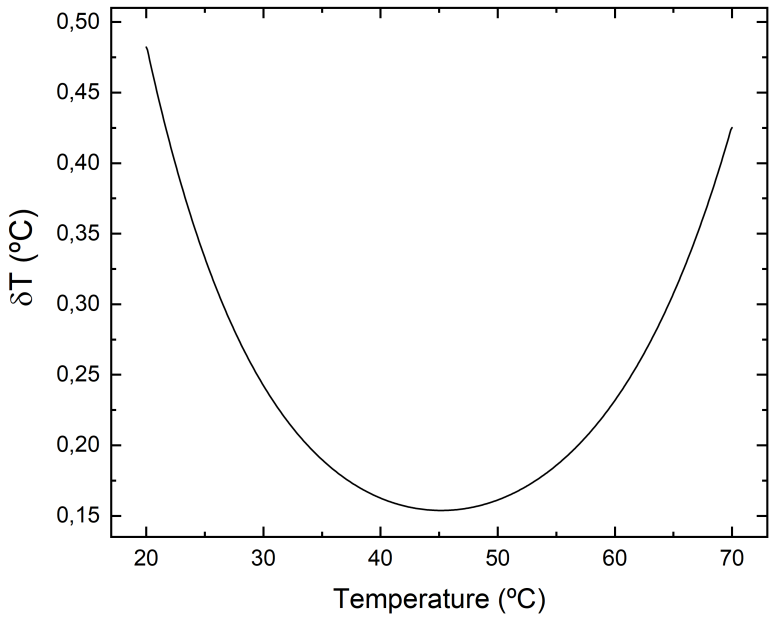

Figure 3.8: Theoretical estimation of the temperature resolution δT in the measured range.

The two methods used to estimate the temperature uncertainty show the same trend with the temperature increase, which makes sense with the relative sensitivity dependence. However, at 40 and 60^{o}C the experimental measure gives a major error than the theoretical calculation of δT, being the experimental value more reliable than the other. However, in both calculations an uncertainty below 0.5^{o}C is achieved in all the measured range, proving the reliability of the sensor with a good value compared to other ratiometric systems [19], [28], [31]. In biological systems, temperature changes as low as 1^{o}C are relevant for the system's properties, so temperature resolution must be on the order of 0.2^{o}C [1], which is achieved in one of the two estimations, but can be improved in future works.

Chapter 4

Conclusions

RESUMEN: En este apartado se resumen las conclusiones en base a los resultados obtenidos. Los objetivos propuestos en el trabajo se cumplen, pues se obtienen partículas fluorescentes cuya caracterización óptica nos permite usar como sensores de temperatura, obteniendo una buena sensitividad y estimaciones del error de medición. Sin embargo, la preparación para su uso en aplicaciones biológicas implicaría futuros estudios más allá del alcance del trabajo.

The possibility of developing a ratiometric thermal nanosensor encapsulating two organic dyes, FITC and Rhodamine B, into silica nanoparticles and its viability for biosensing applications were studied in this work.

Silica nanoparticles with mesoporous core-shell structure were synthesized, obtaining a size between 150-200 nm. The particle size has not been discussed much in the work, however, it would be a factor to consider when it comes to its possible application, as the size is one of the factors that influence the biocompatibility of the particles. However, the synthesis applied permits a size control changing the amount of TEOS or the reaction time.

Furthermore, the absorption and emission spectra permit the verification of the encapsulation of rhodamine B within the pores of the particles and the anchoring of the FITC molecules to the surface with APTES. The potential application of the system as a ratiometric temperature nanosensor in the biological range was investigated by computing the variation in fluorescence intensity of the two compounds, both showing a strong temperature dependence. The results demonstrate a maximum relative sensitivity of $2.91\%^{\circ}C^{-1}$ with an uncertainty of 0.34-0.42ºC over the entire range studied, values that are suitable for use in a temperature sensor with these characteristics. Considering these, the fact that the measurements were taken in an aqueous medium and the biocompatibility of the dyes and the particles, makes them promising for biological and medical applications.

4.1 Future work proposals

Despite the good results obtained in the study, this work only demonstrates the possibility of obtaining a thermal sensor with the characteristics described and the advantages that it would bring. However, before it can be used in the applications described, various factors should be investigated in future projects. This section discusses improvement methods that could be applied for further expansion of the study, as well as other techniques that may be of interest in optimizing the sensor and preparing it for use in biomedical applications.

Firstly, another technique such as Dynamic Light Scattering (DLS) could have been used to characterize the particles, and High Resolution X-Ray Diffraction (HR-XRD) or BET mesurements to determine their exact size and their pore size. To check the functionalization, Fourier-Transform Infrared Spectroscopy could be applied, identifying the molecular vibration presents. These are fingerprints of the available surface molecules and/or the Z potential that could be done with the DLS equipment. This would allow to measure the change in surface charge upon functionalization. In order to provide a complete picture, these experiments would be done after each functionalization step.

An emission study could also be done by varying the concentration of the compounds added to the particles, to see which has the best performance. Another suggestion would be to study the different emission spectra by varying the concentration of particles in the solution with water.

For future studies, modifying the synthesis to directly obtain particles with a mesoporous core structure could be tried. This would allow the two compounds to be encapsulated within the pores, ensuring that energy transfer from one dye to the other takes place by FRET [19], making the fluorescence behavior more predictable.

Furthermore, it is important to emphasize the importance of making measurements with the particles suspended in different aqueous solutions of different pH and viscosity. This is necessary to study the behavior of the sensor in different environments, as it is known that FITC emission is pH dependent. Performing this study should be the next step to focus this sensor on biological applications. Nevertheless, the herein designed and presented sensor is ideal to emulate a system with multiple, input like temperature and pH, and could be exploited to study the feasibility for a single sensor for both local temperature and pH sensing.

Another promising design would be to add a superparamagnetic core. By applying an

external magnetic field with high frequency [34] or infrared light [35] produces local heating and the temperature could be simultaneously readout and locally pinpointed (confocal microscopy in vitro or MRI in vivo). Being able to apply therapy, like hyperthermia in which cancer cells are destroyed at temperature around or above 45 degrees, shrinking tumors, and providing simultaneously a diagnostic system, therefore, it would be a good candidate to design such a theragnostic agent [36].

Bibliography

[1] Jaque, D., & Vetrone, F. (2012). Luminescence nanothermometry. *Nanoscale, 4(15)*, 4301-4326.

[2] Zohar, O., Ikeda, M., Shinagawa, H., Inoue, H., Nakamura, H., Elbaum, D., ... & Yoshioka, T. (1998). Thermal imaging of receptor-activated heat production in single cells. *Biophysical journal, 74(1)*, 82-89.

[3] Karnebogen, M., Singer, D., Kallerhoff, M., & Ringert, R. H. (1993). Microcalorimetric investigations on isolated tumorous and non-tumorous tissue samples. *Thermochimica acta, 229*, 147-155.

[4] Jaque, D., Maestro, L. M., Escudero, E., Rodríguez, E. M., Capobianco, J. A., Vetrone, F., ... & Sole, J. G. (2013). Fluorescent nano-particles for multi-photon thermal sensing. *Journal of luminescence, 133,* 249-253.

[5] Bednarkiewicz, A., Marciniak, L., Carlos, L. D., & Jaque, D. (2020). Standardizing luminescence nanothermometry for biomedical applications. *Nanoscale, 12(27)*, 14405-14421.

[6] Zhou, J., Del Rosal, B., Jaque, D., Uchiyama, S., & Jin, D. (2020). Advances and challenges for fluorescence nanothermometry. *Nature methods, 17(10)*, 967-980.

[7] Wang, X. D., Wolfbeis, O. S., & Meier, R. J. (2013). Luminescent probes and sensors for temperature. *Chemical Society Reviews, 42(19)*, 7834-7869.

[8] Kiyose, K., Kojima, H., Urano, Y., & Nagano, T. (2006). Development of a ratiometric fluorescent zinc ion probe in near-infrared region, based on tricarbocyanine chromophore. *Journal of the American Chemical Society, 128(20)*, 6548-6549.

[9] Falcao, S. J. (2021). *Nanosensores y sistemas inteligentes de liberación controlada basados en nanomateriales porosos* (Doctoral dissertation, Universidad Complutense de Madrid).

[10] Huang, Y., Li, P., Zhao, R., Zhao, L., Liu, J., Peng, S., ... & Zhang, Z. (2022). Silica nanoparticles: Biomedical applications and toxicity. *Biomedicine & Pharmacotherapy, 151*, 113053.

[11] Martínez-Carmona, M., Lozano, D., Colilla, M., & Vallet-Regí, M. (2018). Lectin-conjugated pH-responsive mesoporous silica nanoparticles for targeted bone cancer treatment. *Acta biomaterialia, 65*, 393-404.

[12] Liu, X., Situ, A., Kang, Y., Villabroza, K. R., Liao, Y., Chang, C. H., ... & Meng, H. (2016). Irinotecan delivery by lipid-coated mesoporous silica nanoparticles shows improved efficacy and safety over liposomes for pancreatic cancer. *ACS nano, 10(2)*, 2702-2715.

[13] Hayes, R., Ahmed, A., Edge, T., & Zhang, H. (2014). Core–shell particles: Preparation, fundamentals and applications in high performance liquid chromatography. *Journal of chromatography A, 1357*, 36-52.

[14] Ye, T. X., Du, Y. Y., He, C. Y., Qiu, B., Wang, Y. R., & Chen, X. (2012). Preparation of novel core-shell silica particles for pH sensing using ratiometric fluorescence approach. *Analytical methods, 4(4)*, 1001-1004.

[15] Burns, A., Ow, H., & Wiesner, U. (2006). Fluorescent core–shell silica nanoparticles: towards "Lab on a Particle" architectures for nanobiotechnology. *Chemical Society Reviews, 35(11)*, 1028-1042.

[16] Soleilhac, A., Girod, M., Dugourd, P., Burdin, B., Parvole, J., Dugas, P. Y., ... & Antoine, R. (2016). Temperature response of rhodamine B-doped latex particles. *From solution to single particles. Langmuir, 32(16)*, 4052-4058.

[17] Zhang, Y., Hou, D., & Yu, X. (2020). Facile preparation of FITC-modified silicon nanodots for ratiometric pH sensing and imaging. *Spectrochimica Acta Part A: Molecular and Biomolecular Spectroscopy, 234*, 118276.

[18] Liu, H., Maruyama, H., Masuda, T., Honda, A., & Arai, F. (2014). Multi-fluorescent micro-sensor for accurate measurement of pH and temperature variations in micro-environments. *Sensors and Actuators B: Chemical, 203*, 54-62.

[19] Peerzade, S. A. M., Makarova, N., & Sokolov, I. (2021). Ultrabright fluorescent silica nanoparticles for dual ph and temperature measurements. *Nanomaterials, 11(6)*, 1524.

[20] Ma, X., Jannasch, A., Albrecht, U. R., Hahn, K., Miguel-López, A., Schaffer, E., & Sánchez, S. (2015). Enzyme-powered hollow mesoporous Janus nanomotors. *Nano letters, 15(10)*, 7043-7050.

[21] Yoo, J. H., Lee, E. C., Lee, N. Y., & Kim, J. S. (2009). Synthesis and characterization of mesoporous core-shell silica with incorporation of dye. *Molecular Crystals and Liquid Crystals, 504(1)*, 223-230.

[22] Costa, J. A. S., de Jesus, R. A., Santos, D. O., Neris, J. B., Figueiredo, R. T., & Paranhos, C. M. (2021). Synthesis, functionalization, and environmental application of silica-based mesoporous materials of the M41S and SBA-n families: A review. *Journal of Environmental Chemical Engineering, 9(3)*, 105259.

[23] Hussain, H. I., Yi, Z., Rookes, J. E., Kong, L. X., & Cahill, D. M. (2013). Mesoporous silica nanoparticles as a biomolecule delivery vehicle in plants. *Journal of Nanoparticle Research, 15*, 1-15.

[24] Edinburgh Instruments. FLS1000 Photoluminescence Spectrometer. (2023). https://www.edinst.com/products/fls1000-photoluminescence-spectrometer/

[25] Zaidan, A. H., & Yasin, M. (2016). Detection of Rhodamine B levels in distilled water based on displacement sensor using fiber coupler and concave mirror. *Journal of Optoelectronics and Advanced Materials, 18(11-12)*, 988-992.

[26] Jares-Erijman, E. A., & Jovin, T. M. (2003). FRET imaging. *Nature biotechnology, 21(11)*, 1387-1395.

[27] Wu, Y., Liu, J., Ma, J., Liu, Y., Wang, Y., & Wu, D. (2016). Ratiometric nanothermometer based on rhodamine dye-incorporated F127-melamine-formaldehyde polymer nanoparticle: preparation, characterization, wide-range temperature sensing, and precise intracellular thermometry.*ACS applied materials & interfaces, 8(23)*, 14396-14405.

[28] Peng, M., Kaczmarek, A. M., & Van Hecke, K. (2022). Ratiometric thermometers based on rhodamine B and fluorescein dye-incorporated (nano) cyclodextrin metal–organic frameworks. *ACS Applied Materials & Interfaces, 14(12)*, 14367-14379.

[29] Meng, L., Jiang, S., Song, M., Yan, F., Zhang, W., Xu, B., & Tian, W. (2020). TICT-based near-infrared ratiometric organic fluorescent thermometer for intracellular temperature sensing. *ACS applied materials & interfaces, 12(24)*, 26842-26851.

[30] Zhegalova, N. G., Dergunov, S. A., Wang, S. T., Pinkhassik, E., & Berezin, M. Y. (2014). Design of fluorescent nanocapsules as ratiometric nanothermometers. *Chemistry–A European Journal, 20(33)*, 10292-10297.

[31] Kalaparthi, V., Peng, B., Peerzade, S. A. M. A., Palantavida, S., Maloy, B., Dokukin, M. E., & Sokolov, I. (2021). Ultrabright fluorescent nanothermometers. *Nanoscale Advances, 3(17)*, 5090-5101.

[32] Cao, W., Cui, Y., Yang, Y., & Qian, G. (2021). Dyes encapsulated nanoscale metal–organic frameworks for multimode temperature sensing with high spatial resolution. *ACS Materials Letters, 3(9)*, 1426-1432.

[33] Hernández-Álvarez, C., Brito-Santos, G., Martín, I. R., Sanchiz, J., Saidi, K., Soler-Carracedo, K., ... & Runowski, M. (2023). Multifunctional optical sensing platform of temperature, pressure (vacuum) and laser power density: NaYF 4: Gd 3+, Yb 3+, Er 3+ nanomaterial as luminescent thermometer, manometer and power meter. *Journal of Materials Chemistry C, 11(30)*, 10221-10229.

[34] Lu, X., Liu, Q., Wang, L., Jiang, W., Zhang, W., & Song, X. (2017). Multifunctional triple-porous Fe 3 O 4@ SiO 2 superparamagnetic microspheres for potential hyperthermia and controlled drug release. *RSC Advances, 7(51)*, 32049-32057.

[35] Dai, Z., Wen, W., Guo, Z., Song, X. Z., Zheng, K., Xu, X., ... & Tan, Z. (2020). SiO2-coated magnetic nano-Fe3O4 photosensitizer for synergistic tumour-targeted chemo-photothermal therapy. *Colloids and surfaces B: biointerfaces, 195*, 111274.

[36] Xie, J., Lee, S., & Chen, X. (2010). Nanoparticle-based theranostic agents. *Advanced drug delivery reviews, 62(11)*, 1064-1079.